








NEW METHOD FOR BEARING FAULT DIAGNOSIS BASED ON VMD TECHNIQUE

Yahia BOUSSELOUB ¹ , Farida MEDJANI ^{2,*} , Ahmed BENMASSOUD ³ , Taher KEZAI ⁴,
Ali BELHAMRA ¹ , Issam ATTOUI ⁵ 

¹ Laboratory of Electromechanical Systems, Department of Electromechanics, Faculty of Science and Technology, Badji Mokhtar-Annaba University, Annaba, Algeria

² Mathematics and Their Interactions Laboratory, Abdelhafid Boussouf University Center of Mila, Algeria

³ University of Science and Technology Houari-Boumediène, Algeria

⁴ Catholic University of Louvain, Belgium

⁵ Research Center in Industrial Technologies CRTI P.O. Box 64 Cheraga, Algeria

* Corresponding author, e-mail: f.medjani@centre-univ-mila.dz

Abstract

Variational Mode Decomposition (VMD) is a useful tool for decomposing complex multi-component signals. However, one major drawback of VMD is the need to accurately determine the value of sub-signals (IMFs) before starting the process of segmentation. In fact, achieving optimal reconstruction of the denoised original signals depends on the determining optimal number of IMFs (K). This requirement poses a challenge in the capability of analyzing non-stationary or noisy signals. In this paper, a new approach to optimize the variational mode decomposition technique is proposed. This approach automatically estimates the optimal K and also effectively detects the characteristic frequencies associated with faulty bearings. This method is a combination of two algorithms which are based on cross-correlation and root mean square (RMS) statistical analysis. To confirm the efficacy of the proposed method, the bearing vibration dataset from the Case School of Engineering are used. Then, the K obtained through the proposed method are compared with other methods. The results demonstrate that the proposed approach exhibits superior robustness and precision when autonomously evaluating the optimal K for effective identification of bearing fault.

Keywords: Bearing fault diagnosis, cross correlation, root mean square, vibration signal, variational mode decomposition.

List of Symbols/Acronyms

ADMM – Alternate Direction Method of Multipliers;
CFSA – Center Frequency Statistical Analysis;
DCNN – Deep Convolutional Neural Network;
EMD – Empirical Mode Decomposition;
EK – Envelope Kurtosis;
FIVMD – Fault Information Guided VMD;
FBE – Frequency Band Entropy;
HT – Hilbert Transform;
IVMD – Improved Variational Mode Decomposition;
IVMD – TEO – Improved Variational Mode;
Decomposition and Teager Energy Operator;
LMD – Local Mean Decomposition;
MCFO – Maximum Center Frequency Observation;
OVMD – Optimized Variational Mode Decomposition;
RMS – Root Mean Square;
STFT – Short Time Fourier Transform;
SDA – Signal Difference Average;
SVM – Support Vector Machine;
VMD – Variational Mode Decomposition;
WT – Wavelet Transform.

1. INTRODUCTION

Bearing represent a significant concern in rotating machinery, as a majority of mechanical failures are attributed to bearing-related issues. Consequently, early detection and analysis of bearing faults have become a major focus of scientific research in recent decades. Vibration signal analysis is the most commonly used technique in industry, with approximately 75% of machine diagnostics relying on these signals [1]. However, the signals obtained from these machines are often complex comprising multiple components.

To overcome the complexity of these signals and improve the effectiveness of diagnosing rotating machinery, various signal decomposition methods have been employed in the time-frequency domain. These methods include Short Time Fourier Transform (STFT) [2, 3], Wavelet Transform (WT) [4], Empirical Mode Decomposition (EMD) [5], Ensemble Empirical Mode Decomposition (EEMD) [6], and Local Mean Decomposition (LMD) [7, 8].

However, these methods are often challenged by different issues such as mode mixing and end effects [9]. YU et al. [10] proposed a bearing fault diagnosis method based on Empirical Mode Decomposition (EMD) and Hilbert Transform (HT) techniques. They utilized orthogonal Wavelet Transform bases to translate vibration signals into a time-scale representation. The results show that the proposed method can extract the fault characteristics of roller bearings with high precision.

Recently, the Variational Mode Decomposition (VMD) technique, introduced by Dragomiretskiy and Zosso [11], has gained prominence. VMD can decompose a multi-component signal into a set of intrinsic mode functions (IMFs). One of the main challenges in the VMD algorithm lies in determining the optimal value of K . Nevertheless, in industrial settings, estimating the appropriate K can present significant challenges due to elevated background noise, irregular pulse patterns, and vibrations originating from various internal components. Therefore, research efforts have been directed towards pre-determining and optimizing the K for enhanced diagnostic accuracy. Developing robust methodologies to overcome the challenges associated with estimating the K in industrial environments.

To enhance the operational efficacy of VMD technique, several additional approaches have been proposed. Isham et al. [12] introduced a mode determination technique based on Signal Difference Average (SDA) to capture similarities in amplitudes between the decomposed modes and the original signal. Yang H, Liu and Zhang [13] addressed the effects of over-segmentation and under-segmentation on VMD results. Ni et al. [14] proposed a novel approach (FIVMD), demonstrating its potential in bearing fault detection. Liu et al. [15] developed a method based on Cross Correlation and Teager Energy Operator (IVMD-TEO). Zheng et al. [16] developed a method in which the selection of VMD modes is based on demodulation envelope, and it is used for bearing faults diagnosis.

Moreover, Tang et al. [17] used the Support Vector Machine method to optimize VMD mode number, showing the effectiveness of their approach in analyzing rolling bearing faults. LI et al. [18] present an optimized VMD based on Envelope Kurtosis (EK) and Frequency Band Entropy (FBE), enabling the optimal selection of IMFs. This approach is used for bearing fault diagnosis with high feasibility. WANG, XU and LIU [19] present bearing fault diagnosis based on Improved VMD (IVMD) and Deep Convolutional Neural Network (DCNN). SHI et al. [20] presented a new diagnosis method called VMD – Scale Space Based hyergram. Liu, Wu and Zhen [21] introduced the Maximum Central Frequency Observation method (MCFO) for estimating the value of K , while Wu et al. [22] proposed the Center Frequency Statistical Analysis technique (CFSA) to accurately estimate the value of K . Despite these advancements, some limitations

persist, such as inadequate consideration of independence between IMF components and the energy level of each IMF.

To address these limitations, this paper introduces a novel approach for bearing fault detection that consists of two algorithms. The first algorithm ensures the independence of all IMFs components within their respective frequency bands by utilizing Cross-Correlation coefficients. The second algorithm, based on Root Mean Squared (RMS) histogram analysis, selects IMFs with relevant information (energy level) to eliminate noise effectively. The experimental findings demonstrate that the suggested method overcomes the limitations of previous approaches, yielding robustness, accuracy, and automatic calculation of K . Additionally, the proposed method effectively resolves mode mixing and over-decomposition problems. Applied to bearing vibration diagnosis, the proposed method not only detects defects automatically but also identifies the frequencies characteristic of each defect type.

The remainder of the paper is organized as follows: In Section 2, the theory behind the proposed method is presented. Section 3 provides comparative studies with MCFO and CFSA methods. Section 4 includes experimental validation of the proposed method. Finally, Conclusions are given in Section 5.

2. METHODS AND MATERIALS

2.1. Bearing vibration dataset description

The Electrical Engineering Laboratory of CWRU provided the database [23], based on the experimental test rig presented in Figure 1 which has been used in this study.

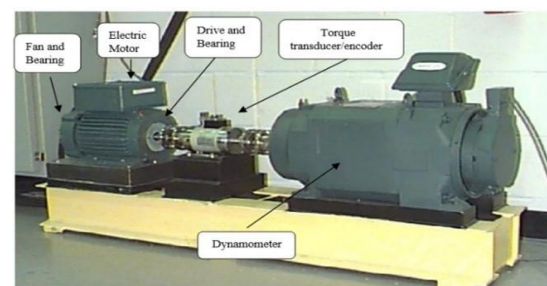


Fig. 1. Experimental test rig [23]

The experimental setup consists of a 2 hp motor, a torque sensor/encoder, a dynamometer, and control electronics. In this study, the vibration signals from the drive end bearing have been measured. The specific type of rolling bearing used in this application is the SKF 6205-2RS JEM. Below are the main characteristics of the healthy and faulty bearing vibration signals from the CWRU dataset, which have been selected for this study [23]:

- The vibration signals are collected at frequency sampling equal to 48,000 Hz and at an operating speed of 1772 rpm.

- Both healthy and faulty signals have been divided into windows of 25ms duration for each recording.
- For the faulty state signals, the fault diameter is 0.177 mm.

Rolling elements generate shock impulses when they encounter localized faults within the inner race with a specific frequency, often referred to as the fault characteristic frequency.

2.2. Variational mode decomposition algorithm

The VMD method can decompose an input signal into an ensemble of intrinsic Mode Functions (IMFs) that can be used to reproduce the original signal. Each IMF has a characteristic center frequency. The resulting constrained variational problem is the following:

$$\min_{u_k, \omega_k} \left\{ \sum_k \left\| \partial_t \left[\left(\delta(t) + \frac{j}{\pi t} \right) * u_k(t) \right] e^{-j\omega_k t} \right\|_2^2 \right\} \quad (1)$$

s. t $\sum_k u_k = f$

The augmented Lagrangian function has been used to solve minimization problem of equation (1).

$$L(\{u_k\}, \{\omega_k\}, \lambda) := \alpha \sum_k \left\| \partial_t \left[\left(\delta(t) + \frac{j}{\pi t} \right) * u_k(t) \right] e^{-j\omega_k t} \right\|_2^2 + \|f(t) - \sum_k u_k(t)\|_2^2 + \langle \lambda(t), f(t) - \sum_k u_k(t) \rangle \quad (2)$$

The resulting IMFs and their corresponding center frequencies are presented as follows:

$$\widehat{u}_k^{n+1}(\omega) = \frac{\widehat{f}(\omega) - \sum_{i < k} \widehat{u}_i^{n+1}(\omega) - \sum_{i > k} \widehat{u}_i^n(\omega) - \frac{\lambda^n(\omega)}{2}}{1 + 2\alpha(\omega - \omega_k^n)^2} \quad (3)$$

$$\omega_k^{n+1} = \frac{\int_0^{+\infty} \omega |\widehat{u}_k^{n+1}(\omega)|^2 d\omega}{\int_0^{+\infty} |\widehat{u}_k^{n+1}(\omega)|^2 d\omega} \quad (4)$$

VMD algorithm details can be found in [11].

2.3. VMD K-value effect in bearing vibration analysis

The over-decomposition and under-decomposition occur when the value of K is greater or less than the actual harmonic number in the input signal, respectively. The aim of this section is to demonstrate and explain the issues of VMD in the decomposition results, such as over-decomposition and mode mixing. Therefore, in the faulty state of the bearing, the modes have been extracted using the VMD algorithm. To this end, when the value of K equals 7, the problem of over-decomposition can be clearly observed in Figure 2.

One can observe that IMF4, IMF6, and IMF7 have very small amplitude levels over their frequency bandwidth compared to IMF1, IMF2, IMF3, and IMF5. Hence, it can be concluded that IMF4, IMF6, and IMF7 are over-decomposed modes and can be regarded as integral components of the residual signal (noise). This noise can be eliminated without any loss of valuable information.

In the healthy state of the bearing, with the same mode number $K=7$, both over-decomposition and mode mixing are clearly observed in Figure 3. Specifically, IMF5, IMF6, and IMF7 have very

small amplitude levels over their frequency bandwidth compared to IMF1, IMF2, IMF3, and IMF4. Hence, these three modes are considered as part of the residual signal and can be dropped without any loss of valuable information (noise). However, IMF3 and IMF4 have the same center frequency with significant amplitudes, indicating the occurrence of the overlapping problem (mode mixing). It can be concluded that $K=7$ is not optimal and only 3 modes (IMF1, IMF2, and IMF3) should be considered in this case. This emphasizes the importance of K in the accuracy of the decomposition.

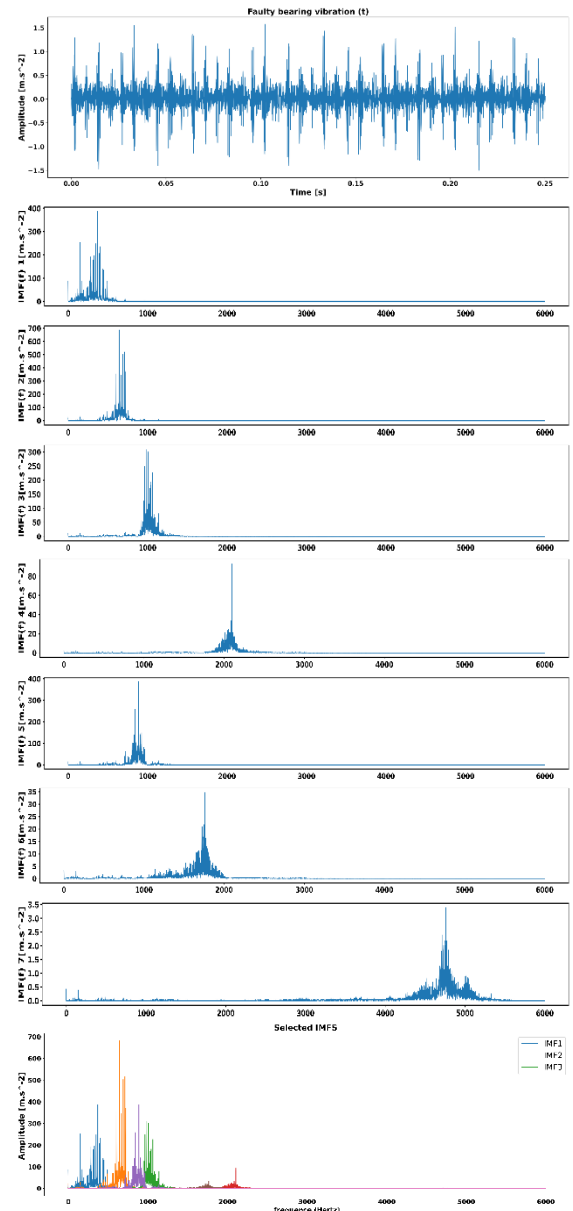


Fig. 2. Modes extracted using VMD for faulty bearing in frequency domain with $K = 7$

2.4. The proposed method

To achieve an automated implementation of the proposed method, it is necessary to enhance the VMD algorithm by incorporating novel constraints.

The proposed method includes two algorithms. The first one, which improves VMD based on Cross-Correlation Coefficients, has been used to ensure that all IMFs are independent in the frequency band. Therefore, three correlation conditions are implemented to automatically estimate the optimal value of K for any input signal and overcome VMD limitations. The first condition ensures that there is no over-decomposition of the residual signal. In fact, when the residue has no more important information, the decomposition stops. However, the second and third conditions are primarily added to avoid the problem of mode duplication.

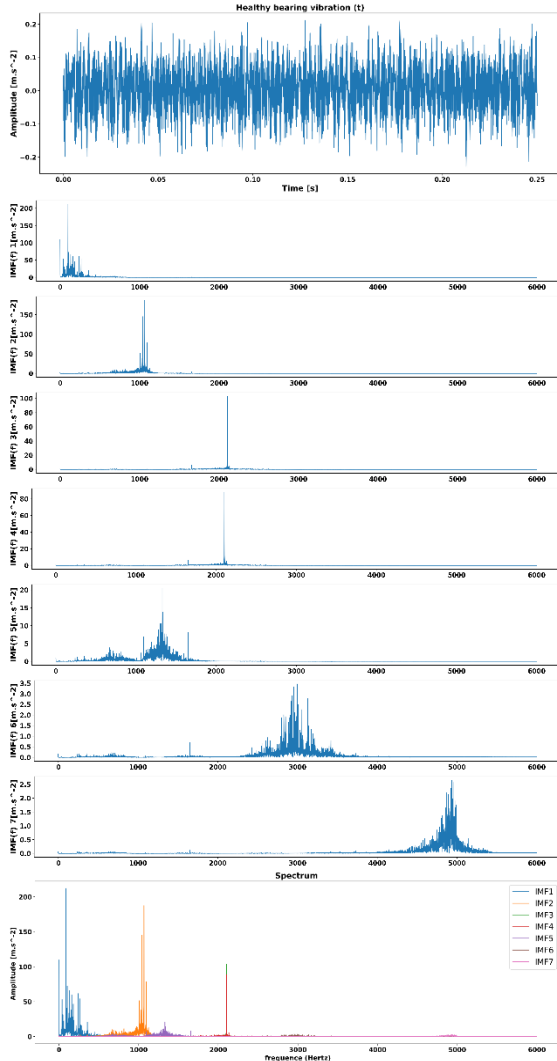


Fig. 3. Modes extracted using VMD for healthy bearing in frequency domain with $K=7$

The second algorithm, based on the Root Mean Square (RMS) method, has been used to select IMFs with relevant information (energy level).

For the first algorithm, three conditions are applied as following:

- The Correlation Coefficient between the input signal and the residual signal must be less than a threshold value of 0.05, as determined through experimental evaluation.

- The Correlation Coefficient of each calculated IMF_i (ith Intrinsic Mode Function) with its next IMF_{i+1} must be lower than a threshold value of 0.1, evaluated experimentally.
- Finally, the correlation of each IMF_i with the original signal must be greater than the correlation of the IMF_i with its next IMF_{i+1} .

Following are the implementation steps of this algorithm:

Algorithm 1: VMD optimization based on CC

- (1) Initialize $k=2$;
- (2) Do₁: $K = k + 1$;
- (3) Initialize $\{\hat{u}_k^1\}, \{\omega_k^1\}, \hat{\lambda}^1, n = 0$
- (4) Do₂: $n = n + 1$;
- (5) **for** $k = 1: K$,

Update \hat{u}_k^{n+1} and ω_k^{n+1} :

$$\hat{u}_k^{n+1}(\omega) = \frac{\hat{f}(\omega) - \sum_{i < k} \hat{u}_i^{n+1}(\omega) - \sum_{i > k} \hat{u}_i^n(\omega) - \frac{\hat{\lambda}^n(\omega)}{2}}{1 + 2\alpha(\omega - \omega_k^n)^2}$$

$$\omega_k^{n+1} = \frac{\int_0^{+\infty} \omega |\hat{u}_k^{n+1}(\omega)|^2 d\omega}{\int_0^{+\infty} |\hat{u}_k^{n+1}(\omega)|^2 d\omega}$$

- (6) Dual ascent:

$$\hat{\lambda}^{n+1}(\omega) = \hat{\lambda}^n(\omega) + \tau(\hat{f}(\omega) - \sum_k \hat{u}_k^{n+1}(\omega));$$

- (7) **repeat** steps (4)-(6), **until**

$$\sum_k \frac{\|\hat{u}_k^{n+1} - \hat{u}_k^n\|_2^2}{\|\hat{u}_k^n\|_2^2} < \epsilon;$$

- (8) **for** $k=1: K$,

$$r_1 = r(u_i, u_{i+1})$$

$$r_2 = r(u_i, f)$$

if $r_1 > 0.1$ stop decomposition and number of modes is $K-1$;

elif $r_1 > r_2$ stop decomposition and number of modes is $K-1$;

- (9) **repeat** steps (2)-(8), **until**

$$|r(f - \sum u_k, f)| < \sigma, \text{ with } \sigma = 0.09.$$

The aim of the second algorithm IVMD is to compare the amplitudes of each IMF by calculating their RMS values. This method calculates the average power of each IMF over a given period and represents a useful tool for comparing the energy of different signals or assessing the signal's power.

Therefore, only IMFs that have an energy level above the computed RMS threshold are selected. It's assumed that the omitted modes lack sufficient information to influence the process of fault detection and identification. The process of selecting useful IMFs within the original signal can be summarized as follows:

1. Calculate RMS for each IMF.
2. Estimate the expected amplitude percentage of each mode compared to the IMF with the largest RMS value.
3. Calculate the threshold (noted γ).
4. Select the IMFs that have higher RMS value than the threshold

Following are the implementation steps of the second algorithm:

Algorithm 2: IMFs selection based on RMS

(1) **for** $k = 1: K$,

$$rms_k = \sqrt{\frac{(IMF_k[0]^2 + IMF_k[1]^2 + IMF_k[2]^2 + \dots + IMF_k[n]^2)}{n}}$$

(2) Find rms_{max} the largest value among rms values;

(3) Estimate the expected amplitude percentage of each mode;

$$rms_k(\%) = \frac{rms_k \times 100}{rms_{max}};$$

(4) Calculate the average;

$$\text{average} = \sum_k \frac{rms_k(\%)}{K};$$

(5) Calculate the threshold;

$$\gamma = \text{average} \times 0.8;$$

(6) **for** $k=1: K$,

if $rms_k(\%) > \gamma$, IMF_k is a selected mode;
else, drop off all the remained IMFs;

The Optimized VMD algorithm flowchart is presented in Fig 5.

3. COMPARATIVE EXAMINATION BETWEEN PROPOSED APPROACH, MCFO AND CFSA METHODS IN BEARING VIBRATION ANALYSIS

To validate the effectiveness of the proposed method in analyzing bearing vibration, both the Maximum Center Frequency Observation (MCFO) and Center Frequency Statistical Analysis (CFSA) algorithms have been implemented in this study for comparison purposes.

3.1. MCFO method

The MCFO approach relies on examining the pattern displayed by the highest center frequencies. The center frequency of each IMF gradually increases as the mode number increments. The point at which the maximum center frequencies exhibit stability corresponds to the identification of the optimal value of K [21]. The application of this method to the simulated signal equation (5).

$$f(t) = 0.1 * \cos(2\pi 100t) + 2 * \cos(2\pi 350t) + 0.4 \cos(2\pi 400t) + \cos(2\pi 800t) + \cos(2\pi 950t) \quad (5)$$

The optimal number of modes in this case should be $K=5$

From Figure 4 it can be observed that as the number of modes increase, the corresponding center frequencies gradually increases and tend to be stabilize at $K=5$, Therefore, the optimal value of K is 5.

3.2. CFSA method

The main idea behind the CFSA method is to count the frequencies in the histogram that surpass the mean value [22]. This selected number is

considered as the optimal mode number. The implementation steps of the algorithm are as follows:

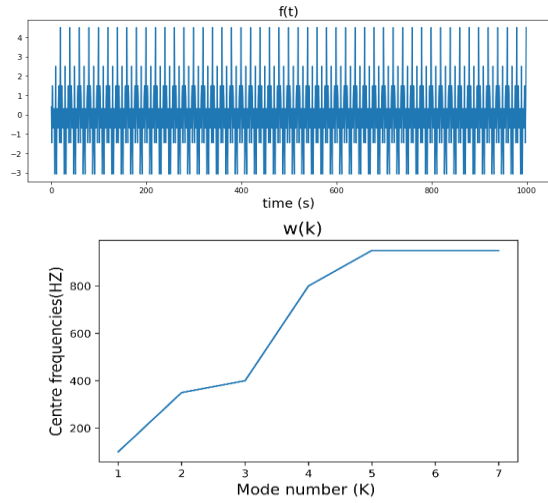


Fig. 4. MCFO of simulated signal $f(t)$

Algorithm 3: CFSA algorithm

(1) Initialize VMD parameters (k, α).

(2) Extract IMFs of the input signal using VMD.

(3) Estimate the center frequency of each IMF.

(4) Plot the histogram of center frequencies.

(5) Determine the mean of central frequencies and count number (N) exceeding the average.

(6) **repeat** steps (1)-(5) with ($k = k + 1$), **until** the incrementation of the count number has ceased, the decomposition is stopped, the optimal value of IMF is N .

3.3. Results and discussion

A Python program for the MCFO and CFSA methods for comparative analysis with the proposed approach have been developed from scratch.

First, the CFSA algorithm is applied to the healthy signal, and the resulting center frequency histogram is shown in Figure 6. Dominant center frequencies that are above the average count of 3.66 are: 113 Hz, 1044 Hz, 1297 Hz, 2099 Hz, and 4889 Hz. According to the CFSA method, the original signal has only 5 optimal IMFs as main components. In faulty state condition, the center frequency histogram is shown in Figure 7, with an average count of 4.88. The dominant center frequencies are: 325 Hz, 666 Hz, 845 Hz, and 2075 Hz. Hence, there are four frequencies, thus 4 IMFs, that can be considered as optimal components of the faulty original signal.

The results of the application of the MCFO method are shown in Figures 8 and 9, for healthy and faulty signals respectively. As seen in Figure 8, the center frequency stabilizes when $K=3$, indicating that the optimal number of IMF is 3. However, in Figure 9, the maximum center frequency tends to stabilize from $K=6$, indicating that the optimal number of IMFs is 6.

The proposed method is used to process both healthy and faulty states of the signal, and the

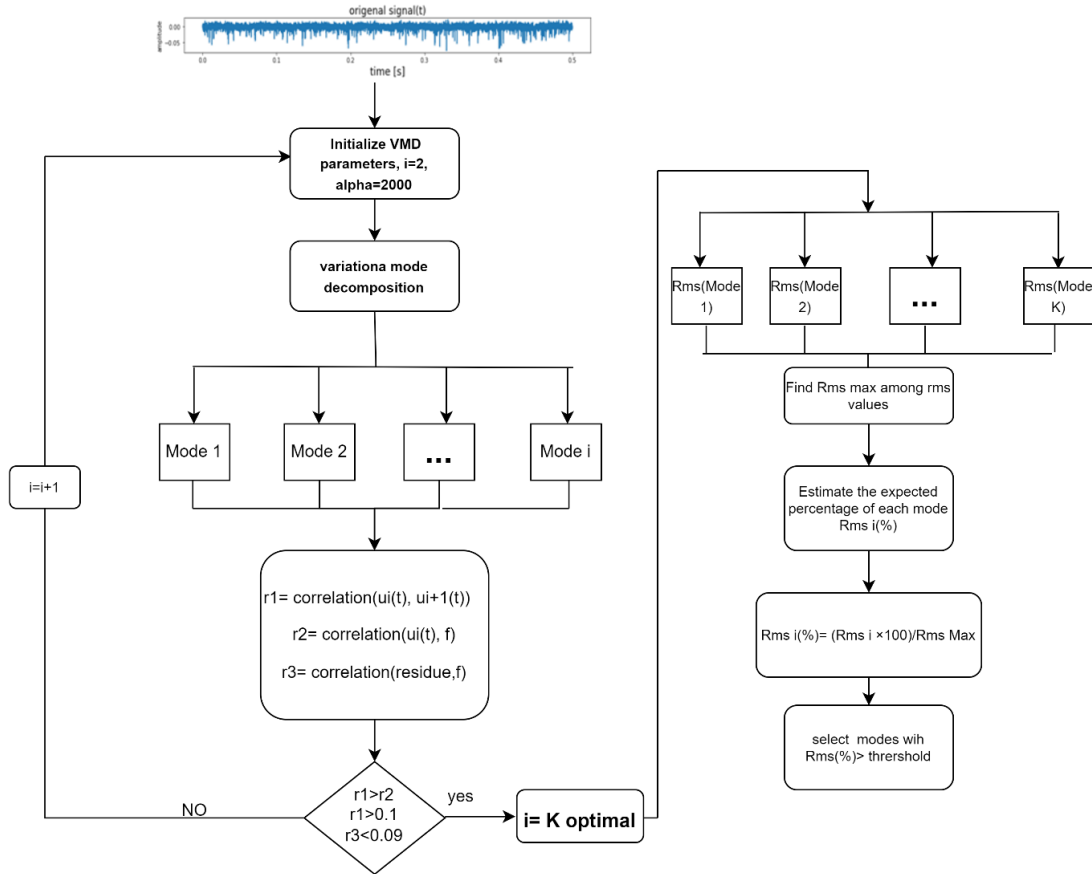


Fig. 5. The method presented in this paper

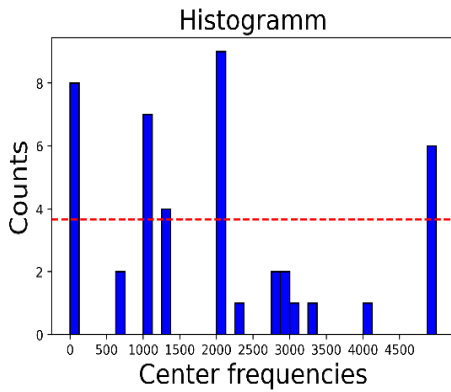


Fig. 6. Center Frequency Histogram for healthy state (Counts average = 3.66)

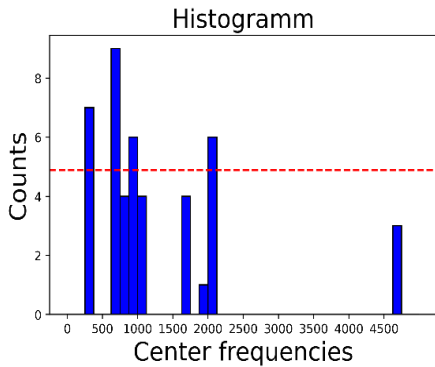


Fig. 7. Center Frequency Histogram for faulty state (Counts average = 4.88)

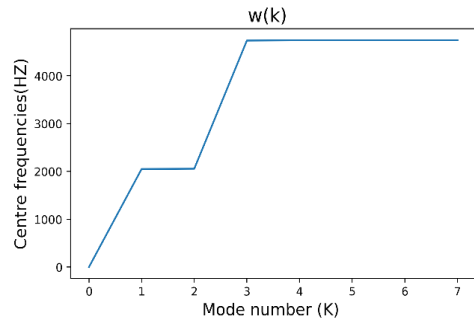


Fig. 8. MCFA trend of bearing vibration signal in healthy state

computed value of K for all previous methods are summarized in Table 1.

Table 1. The value of K for each method

	Healthy state	Faulty state
MCFO	$K=3$	$K=6$
CFSA	$K=5$	$K=4$
Proposed approach	$K=3$	$K=4$

For the healthy state, both MSFO and the proposed method give $K=3$. However, the CFSA method indicates that the value of K is 5. Figure 10 presents the output of the first algorithm (VMD optimization based on cross-correlation), showing effective suppression of modal aliasing and adaptive

separation of different frequency bands. However, the amplitudes of modes 4 and 5 are very small compared to modes 1, 2, and 3. This means that the two former modes have very limited useful information. Based on the RMS results using second algorithm in Figure 11, it can conclude that IMF4 and IMF5 must be dropped because their energy level is under the threshold of 48.67%. Therefore, the selected IMFs are mode 1, mode 2, and mode 3. The remaining modes have to be dropped, confirming that the optimal value of K extracted by the proposed approach must be equal to 3, as shown in Figure 12.

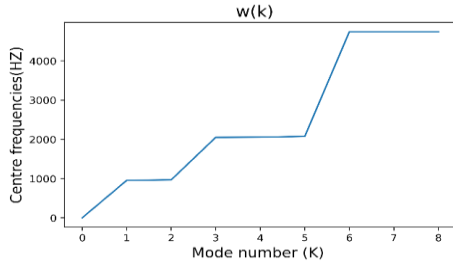


Fig. 9. MCFA trend of bearing vibration signal in faulty state

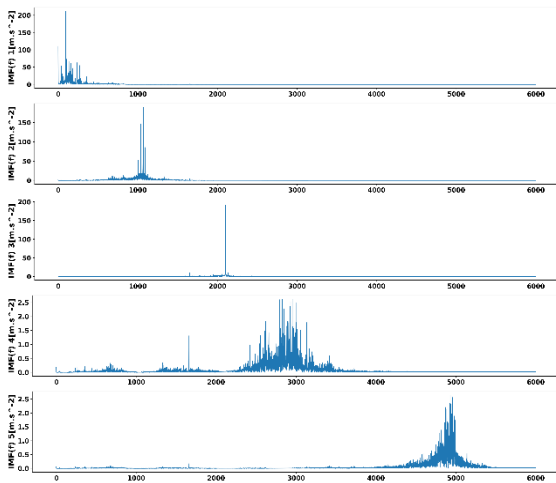


Fig. 10. The output of first algorithm (VMD optimization based on cross correlation) in healthy state

For the faulty state, both CFSA and the proposed approach give a $K=4$. However, the MSFO method indicates that the value of K is 6. Figure 13 presents the decomposition result of the first algorithm (VMD optimization based on cross correlation), where it can be observed that the amplitudes of modes 3 and 6 are very small compared to modes 1, 2, 4, and 5, indicating that the two former modes have very limited useful information.

Indeed, based on the RMS representation of each mode in Figure 14, it can be concluded that IMF3 and IMF6 energies are below the energy threshold level of 57.66%. So, they must be considered as part of the residual signal. This means that the optimal value of K extracted by our approach is equal to 4. Therefore, the selected IMFs are modes 1, 2, 4, and 5. The output of the proposed algorithm for the faulty state is presented in Figure 15.

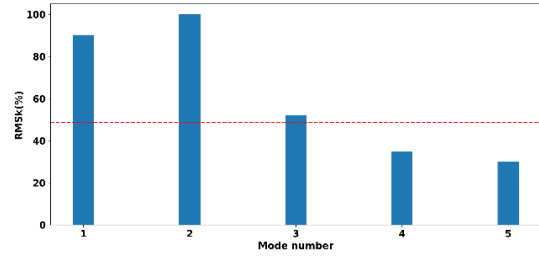


Fig. 11. The RMS representation of each mode with threshold =48.67%

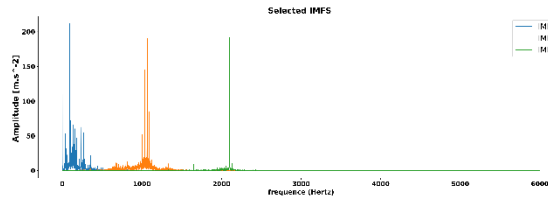


Fig. 12. Modes selected by the proposed method for healthy bearing vibration signal in frequency domain

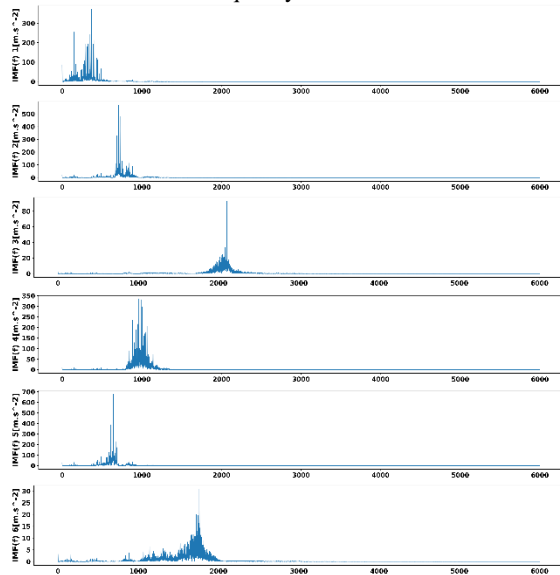


Fig. 13. The output of first algorithm (VMD optimization based on cross correlation) in faulty state

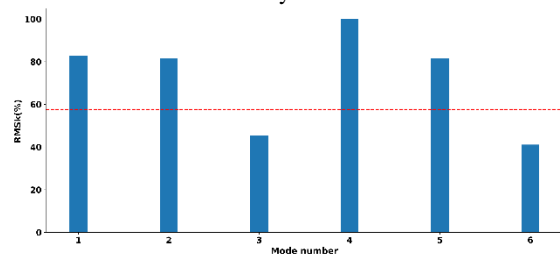


Fig. 14. The RMS representation of each mode with threshold =57.66%

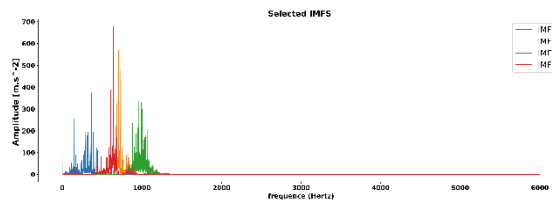


Fig. 15. Modes selected by the proposed method for faulty bearing vibration signal in frequency domain

4. OVMD FOR BEARING FAULT DETECTION AND IDENTIFICATION

The objective of this section is to verify the robustness of the proposed method for bearing fault detection and identification. Furthermore, a key advantage of this method is that the decomposition process and the selection of the optimal value of K are performed automatically, eliminating the requirement for human intervention, as explained in the previous section, analyzing bearing vibration of healthy and faulty (Inner race fault) signals.

The characteristic frequency of inner race fault can be represented as:

$$f_i = BPFi \times \text{Shaft speed}(RPS) = 159.48 \text{ Hz} \quad (6)$$

Table 2. Bearing details and fault frequencies [24]

Fault frequencies (multiple of shaft speed)			
BPFI	BPFO	FTF	BSF
5.415	3.585	0.3983	2.357

The decomposed results of the healthy and faulty bearing signals are shown in Figure 16. It can be concluded that the intensities of IMFs in the faulty state have increased significantly compared to the healthy state. Therefore, the dissimilarities between the faulty and healthy states can be easily distinguished. The characteristic frequency of the inner race fault $f(i) = 159.48 \text{ Hz}$, as well as its harmonics ($2f_i$, $4f_i$, $6f_i$, $8f_i$), are clearly determined. Hence, the inner race fault has not only been detected but also identified, confirming the feasibility and effectiveness of the proposed method.

Table 3. Inner race characteristic frequency and its harmonics

	f_i	$2f_i$	$4f_i$	$6f_i$	$8f_i$
Amplitudes $m \cdot s^{-2}$	250	380	645	345	310
Frequencies Hz	159.48	318.96	637.92	956.88	1278.84

Moreover, to demonstrate the efficacy of the proposed method, we can use it to analyze additional bearing faults, such as outer race and rolling element (ball) faults. From the same Experimental test rig, CWRU dataset [23], the faulty outer race and rolling element vibration signals are presented in Figure 17.

The results of the application of the proposed method on faulty outer race vibration is shown in Figures 18, 19 and 20.

The characteristic frequency of outer race fault can be represented as:

$$f_i = BPF0 \times \text{Shaft speed}(RPS) = 105.87 \text{ Hz} \quad (7)$$

The characteristic frequency of the outer race fault $f(i) = 105.87 \text{ Hz}$, as well as its harmonics ($2f_i$, $3f_i$, $5f_i$, $6f_i$, $7f_i$), are clearly determined and presented in Table 4.

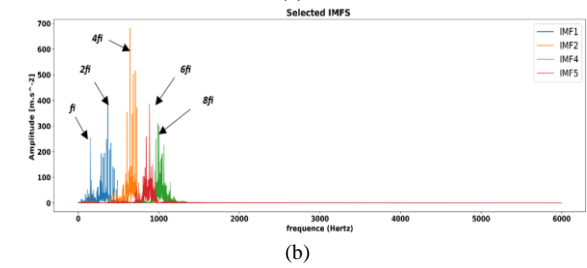
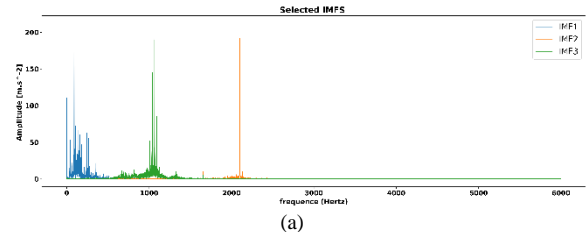


Fig. 16. IMFs selection using OVMD for (a) healthy vibration and (b) Inner race fault vibration

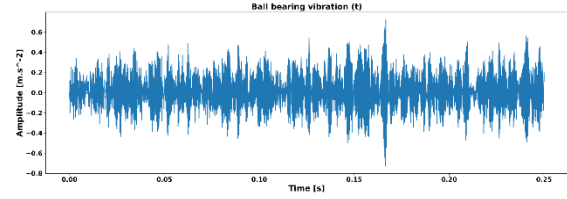
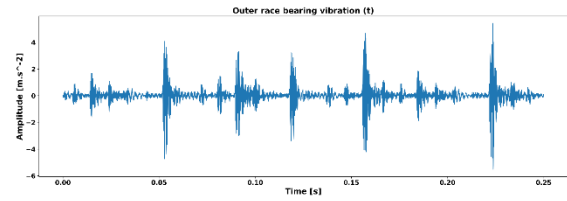


Fig. 17. Outer race and ball bearing vibration signals in Time Domane

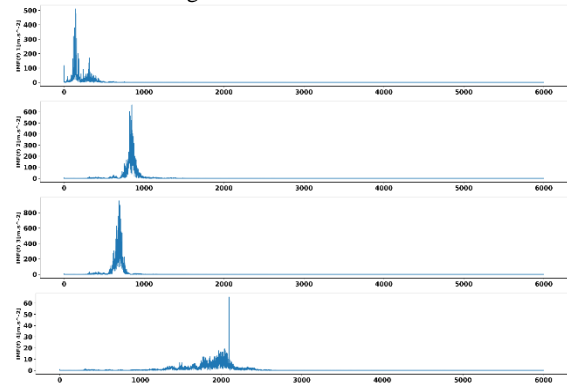


Fig. 18. The output of first algorithm (VMD optimization based on cross correlation) in outer race vibration signal

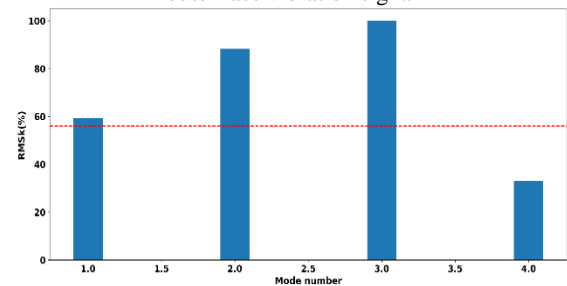


Fig. 19. The RMS representation of each mode with threshold =56.09%

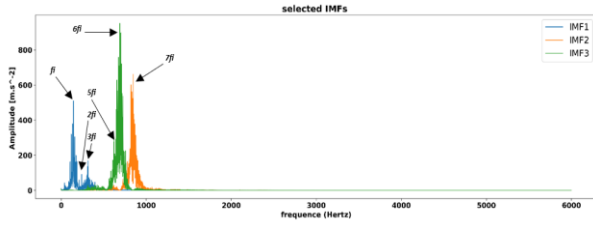


Fig. 20. IMFs selection using OVMD for outer race fault vibration

Table 4. Outer race characteristic frequency and its harmonics

	F_i	$2F_i$	$3F_i$	$4F_i$	$5F_i$
Amplitudes $m.s^{-2}$	65.43	111	56.55	64.95	41.55
Frequencies Hz	69.61	139.22	208.83	278.44	348.05
	$7F_i$	$8F_i$	$9F_i$	$10F_i$	
Amplitudes $m.s^{-2}$	64.86	382.4	382.5	110.56	
Frequencies Hz	487.27	556.88	626.49	696.1	

The results of the application of the proposed method on faulty ball bearing vibration is shown in Figures 21, 22 and 23.

The characteristic frequency of Ball bearing fault can be represented as:

$$f_i = BSF \times \text{Shaft speed}(RPS) = 69.61 \text{ Hz} \quad (8)$$

The characteristic frequency of the Ball bearing fault $f(i) = 69.61 \text{ Hz}$, as well as its harmonics ($2f_i, 3f_i, 4f_i, 5f_i, 7f_i, 8f_i, 9f_i, 10f_i$), are clearly determined and presented in Table 5.

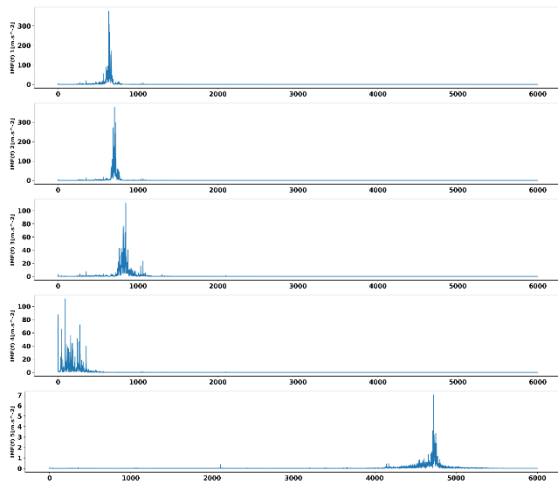


Fig. 21. The output of first algorithm (VMD optimization based on cross correlation) in ball vibration fault

The results show that the proposed method can automatically and significantly select the optimal modes for inner race, outer race and ball bearing vibrations. Moreover, it identifies the characteristic frequencies of each.

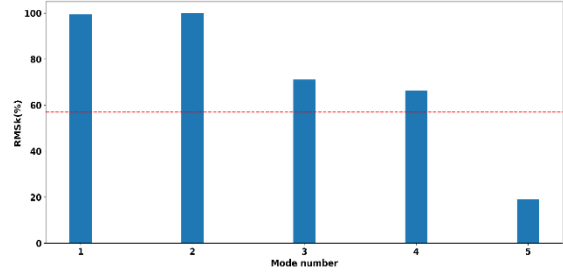


Fig. 22. The RMS representation of each mode with threshold =56.96%

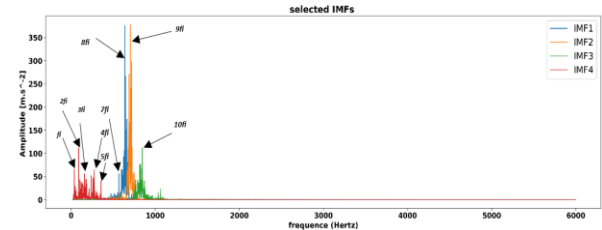


Fig. 23. IMFs selection using OVMD for ball vibration fault

Table 5. The characteristic frequency of the Ball bearing fault and its harmonics

	F_i	$2F_i$	$3F_i$	$5F_i$	$6F_i$	$7F_i$
Amplitudes $m.s^{-2}$	501.03	94.4	175.56	325	960	685.33
Frequencies Hz	105.87	211.74	317.61	529.35	635.22	741.09

5. CONCLUSION

This paper introduces a novel method that enhances the computation of VMD modes that is based on the combination of Cross-Correlation and the RMS algorithms. Through its application to processing vibration signals from rolling bearings, the efficacy of the proposed method becomes evident. When compared to the MCFO and CFSA methods, it is more efficient, robust, and accurate. This method determines the optimal value of K for processing real-world bearing vibration signals, as extracted from the CWRU dataset for Inner race, outer race and ball bearing faults detection and characteristic frequency identification. This showcases its potential for on-the-fly fault diagnosis and identification within industrial settings. Future research will extend the utility of this method to analyzing various types of vibration signals, such as gearboxes, rotors, and stator vibrations.

Acknowledgment: *R&D activities have been realized within Innovation Academy Mila in collaboration with Annaba University and University Center of Mila. the authors are grateful to prof Tahar Kezai president of Innovation Academy for their continue supports and advices.*

Source of funding: *This research received no external funding.*

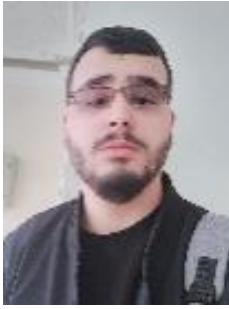
Author contributions: *research concept and design, Y.B., F.M., T.K.; Collection and/or assembly of data, Y.B., T.K.; Data analysis and interpretation, Y.B., F.M., T.K.; Writing*

the article, Y.B., F.M.: *Critical revision of the article*, Y.B., A.B., T.K, F.M.; *Final approval of the article*, A.B., T.K., I.A.

Declaration of competing interest: *The authors declare that they have no known competing financial interests or personal relationships that could have appeared to influence the work reported in this paper.*

REFERENCES

- Gangsar P, Tiwari R. Signal based condition monitoring techniques for fault detection and diagnosis of induction motors: A state-of-the-art review. *Mechanical Systems and Signal Processing* 2020; 144: 106908. <https://doi.org/10.1016/j.ymssp.2020.106908>.
- Qin SR, Zhong YM. Research on the unified mathematical model for FT, STFT and WT and its applications. *Mechanical Systems and Signal Processing* 2004; 18(6): 1335–47. <https://doi.org/10.1016/j.ymssp.2003.12.002>.
- Liu D, Cheng W, Wen W. Rolling bearing fault diagnosis via STFT and improved instantaneous frequency estimation method. *Procedia Manufacturing* 2020; 49: 166–72. <https://doi.org/10.1016/j.promfg.2020.07.014>.
- Yan R, Gao RX, Chen X. Wavelets for fault diagnosis of rotary machines: A review with applications. *Signal Processing* 2014; 96: 1–15. <https://doi.org/10.1016/j.sigpro.2013.04.015>.
- Saidi L, Ali JB, Fnaiech F. Bi-spectrum based-EMD applied to the non-stationary vibration signals for bearing faults diagnosis. *ISA transactions* 2014; 53(5): 1650–60. <https://doi.org/10.1016/j.isatra.2014.06.002>.
- Yeh JR, Shieh JS, Huang NE. Complementary ensemble empirical mode decomposition: a novel noise enhanced data analysis method. *Advances in Adaptive Data Analysis* 2010; 02(02): 135–56. <https://doi.org/10.1142/S1793536910000422>.
- Yongbo LI SS. Review of local mean decomposition and its application in fault diagnosis of rotating machinery. *Journal of Systems Engineering and Electronics* 2019; 30(4): 799–814. <https://doi.org/10.21629/JSEE.2019.04.17>.
- Smith JS. The local mean decomposition and its application to EEG perception data. *Journal of The Royal Society Interface* 2005; 2(5): 443–54. <https://doi.org/10.1098/rsif.2005.0058>.
- Hao R, Li F. A new method to suppress the EMD end point effect, Zhendong Ceshi Yu Zhenduan/Journal of Vibration, Measurement and Diagnosis 2018, 38(2): 341-345.
- Yu D, Cheng J, Yang Y. Application of EMD method and Hilbert spectrum to the fault diagnosis of roller bearings. *Mechanical Systems and Signal Processing* 2005; 19(2): 259–70. [https://doi.org/10.1016/S0888-3270\(03\)00099-2](https://doi.org/10.1016/S0888-3270(03)00099-2).
- Dragomiretskiy K, Zosso D. Variational Mode Decomposition. *IEEE Transactions on Signal Processing* 2014; 62(3): 531–44. <https://doi.org/10.1109/TSP.2013.2288675>.
- Isham MF, Leong MS, Lim MH, Ahmad ZA. Variational mode decomposition: mode determination method for rotating machinery diagnosis. *Journal of Vibroengineering* 2018; 20(7): 2604–21. <https://doi.org/10.21595/jve.2018.19479>.
- Yang H, Liu S, Zhang H. Adaptive estimation of VMD modes number based on cross correlation coefficient. *Journal of Vibroengineering* 2017; 19(2): 1185–96. <https://doi.org/10.21595/jve.2016.17236>.
- Ni Q, Ji JC, Feng K, Halkon B. A fault information-guided variational mode decomposition (FIVMD) method for rolling element bearings diagnosis. *Mechanical Systems and Signal Processing* 2022; 164: 108216. <https://doi.org/10.1016/j.ymssp.2021.108216>.
- Liu S, Tang G, Wang X, He Y. Time-Frequency Analysis Based on Improved Variational Mode Decomposition and Teager Energy Operator for Rotor System Fault Diagnosis. *Mathematical Problems in Engineering* 2016; 2016: e1713046. <https://doi.org/10.1155/2016/1713046>.
- Zheng X, Zhou G, Wang J, Ren H, Li D. Variational mode decomposition applied to offshore wind turbine rolling bearing fault diagnosis. 2016 35th Chinese Control Conference (CCC) 2016 p. 6673–7. <https://doi.org/10.1109/ChiCC.2016.7554407>.
- G Tang, X Wang, Y He, S Liu, rolling bearing fault diagnosis based on variational mode decomposition and permutation entropy, 13th International Conference on Ubiquitous Robots and Ambient Intelligence (URAI), IEEE, 2016: 626-631. <https://doi.org/10.1109/URAI.2016.7625792>.
- Li H, Liu T, Wu X, Chen Q. An optimized VMD method and its applications in bearing fault diagnosis. *Measurement* 2020; 166: 108185. <https://doi.org/10.1016/j.measurement.2020.108185>.
- Wang R, Xu L, Liu F. Bearing fault diagnosis based on improved VMD and DCNN. *Journal of Vibroengineering* 2020; 22: 1055–68. <https://doi.org/10.21595/jve.2020.21187>.
- Shi W, Wen G, Huang X, Zhang Z, Zhou Q. The VMD-scale space based hoyergram and its application in rolling bearing fault diagnosis. *Measurement Science and Technology* 2020; 31(12): 125006. <https://doi.org/10.1088/1361-6501/aba70c>.
- Liu C, Wu Y, Zhen C. Rolling bearing fault diagnosis based on variational mode decomposition and fuzzy C means clustering. *Zhongguo Dianji Gongcheng Xuebao/Proceedings of the Chinese Society of Electrical Engineering* 2015; 35: 3358–65. <https://doi.org/10.13334/j.0258-8013.pcsee.2015.13.020>.
- Wu S, Feng F, Zhu J, Wu C, Zhang G. A Method for Determining Intrinsic Mode Function Number in Variational Mode Decomposition and Its Application to Bearing Vibration Signal Processing. *Shock and Vibration* 2020; 2020: e8304903. <https://doi.org/10.1155/2020/8304903>.
- Case Western Reserve University Bearing Data Center website, 48k Drive End Barking Fault Data | Case School of Engineering | Case Western Reserve University.
- Smith WA, Randall RB. Rolling element bearing diagnostics using the Case Western Reserve University data: A benchmark study. *Mechanical Systems and Signal Processing* 2015; 64–65: 100–31. <https://doi.org/10.1016/j.ymssp.2015.04.021>.

**Yahia BOUSSELOUB**

is a PhD student at the Electromechanical Engineering Laboratory in Badji Mokhtar-Annaba University, starting in 2020. He received his Master's degree in Electromechanics from Abdelhafid Boussouf University Center, Mila, Algeria, in 2020. His primary research interests include predictive maintenance of rotating machinery through

vibration analysis, utilizing advanced signal processing, image processing, and artificial intelligence methods. Additionally, he is interested in industrial automation and control.

e-mail: yahia.bousseloub@univ-annaba.org

**Ali BELHAMRA**

holds the Doctorate degrees in electrical engineering from Badji Mokhtar University, Annaba, Algeria, earned in 2006. Since 2017, he has been a full-time Research Associate at the Electromechanical Engineering Laboratory in Badji Mokhtar-Annaba University, Algeria. Group leader of optimization of

means of transport. His research interests encompass industrial process control, fault diagnosis, renewable energy, and signal processing.

e-mail: belhamraali@yahoo.fr

Farida MEDJANI holds the Doctorate degrees in materials science from Mentouri University, Constantine, Algeria, earned in 2007. Since 2012, she has been a full-time Research Associate at Mathematics and their interactions Laboratory in Abdelhafid Boussouf University Center of Mila, Algeria. Her research interests encompass renewable energy and predictive maintenance using advanced signal processing, image processing, and artificial intelligence methods.

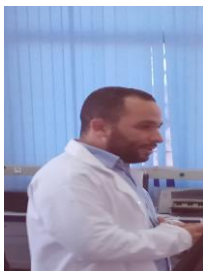
e-mail: f.medjani@centre-univ-mila.dz

**Ahmed BENMESSAOUD**

is a young individual interested in AI development and research in the domains of Gans, computer vision, tinyML. He recently graduate with a master's degree in artificial intelligence from USTHB Algeria. Now, works as a researcher in Innovation Academy Mila in Algeria, as well as, creating a computer vision startup to improve the quality,

productivity, and safety of manual assembly work in the manufacturing industry.

e-mail: ahmed.sif.benmessaoud.13@gmail.com

**Issam ATTOUI**

holds the State Engineer, Magister, and Doctorate degrees in electrical engineering from Badji Mokhtar University, Annaba, Algeria, earned in 2007, 2009, and 2015, respectively. Additionally, he obtained the "Habilitation to supervise research" degree in electrical engineering from 20 août

1955 University, Skikda, Algeria, in 2018. Since July 2011, he has been a full-time Research Associate at the Research Center in Industrial Technologies, Cheraga, Algeria. His research interests encompass industrial process control, fault diagnosis, renewable energy, and signal processing.

e-mail: i.attoui@crti.dz